Electronic Supplementary Information for

Predictable incorporation of nitrogen into carbon dots: Insights from pinacol rearrangement and iminium ion cyclization

Soohyun Cho[a], Chan-Woo Jung[b], Dajin Lee[a], Yerim Byun[a], Hyemin Kim[c], Hyunho Han[d], Ji-Hee Kim*[,e], and Woosung Kwon*[,a,f]

[a]Department of Chemical and Biological Engineering, Sookmyung Women's University, Seoul 04310, South Korea

[b]Department of Energy Science, Sungkyunkwan University, Suwon 16419, South Korea

[c]Department of Cosmetics Engineering, Konkuk University, Seoul 05029, South Korea

[d]Department of Urology, Urological Science Institute, Yonsei University College of Medicine, Seoul 03722, South Korea

[e]Department of Physics, Pusan National University, Busan 46241, South Korea

[f]Institute of Advanced Materials and Systems, Sookmyung Women's University, Seoul 04310, South Korea

*Corresponding author.

wkwon@sookmyung.ac.kr (Woosung Kwon)

kimjihee@pusan.ac.kr (Ji-Hee Kim)

Table of Contents

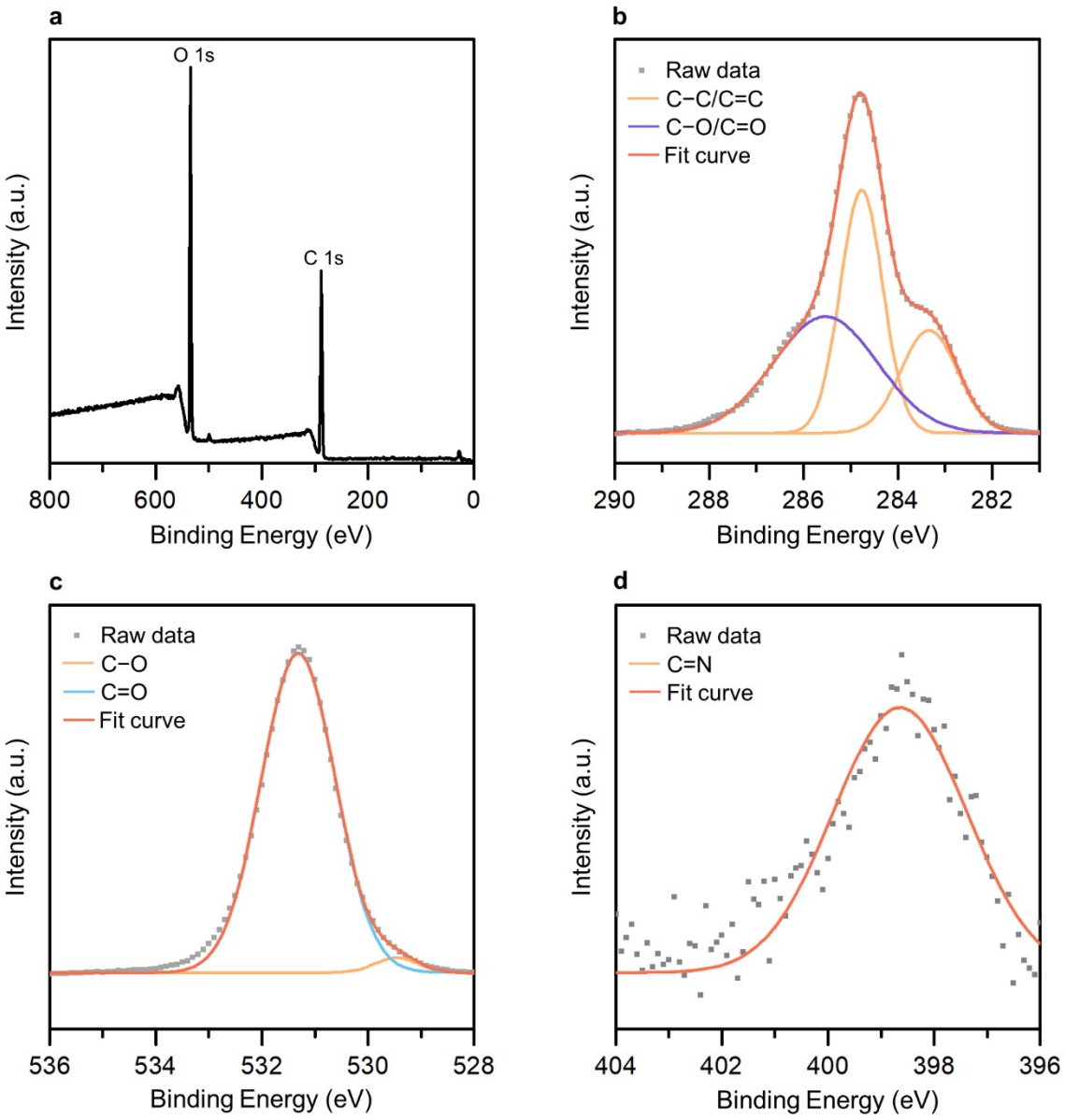

Fig. S1. (a) XPS spectrum of G-CDs. High-resolution XPS spectra of (b) carbon 1s, (c) oxygen 1s, and (d) nitrogen 1s of G-CDs.

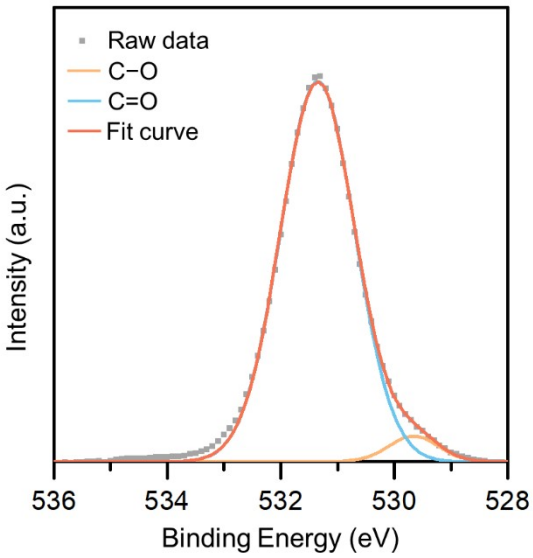

Fig. S2. High-resolution XPS spectra of oxygen 1s of GE-CDs.

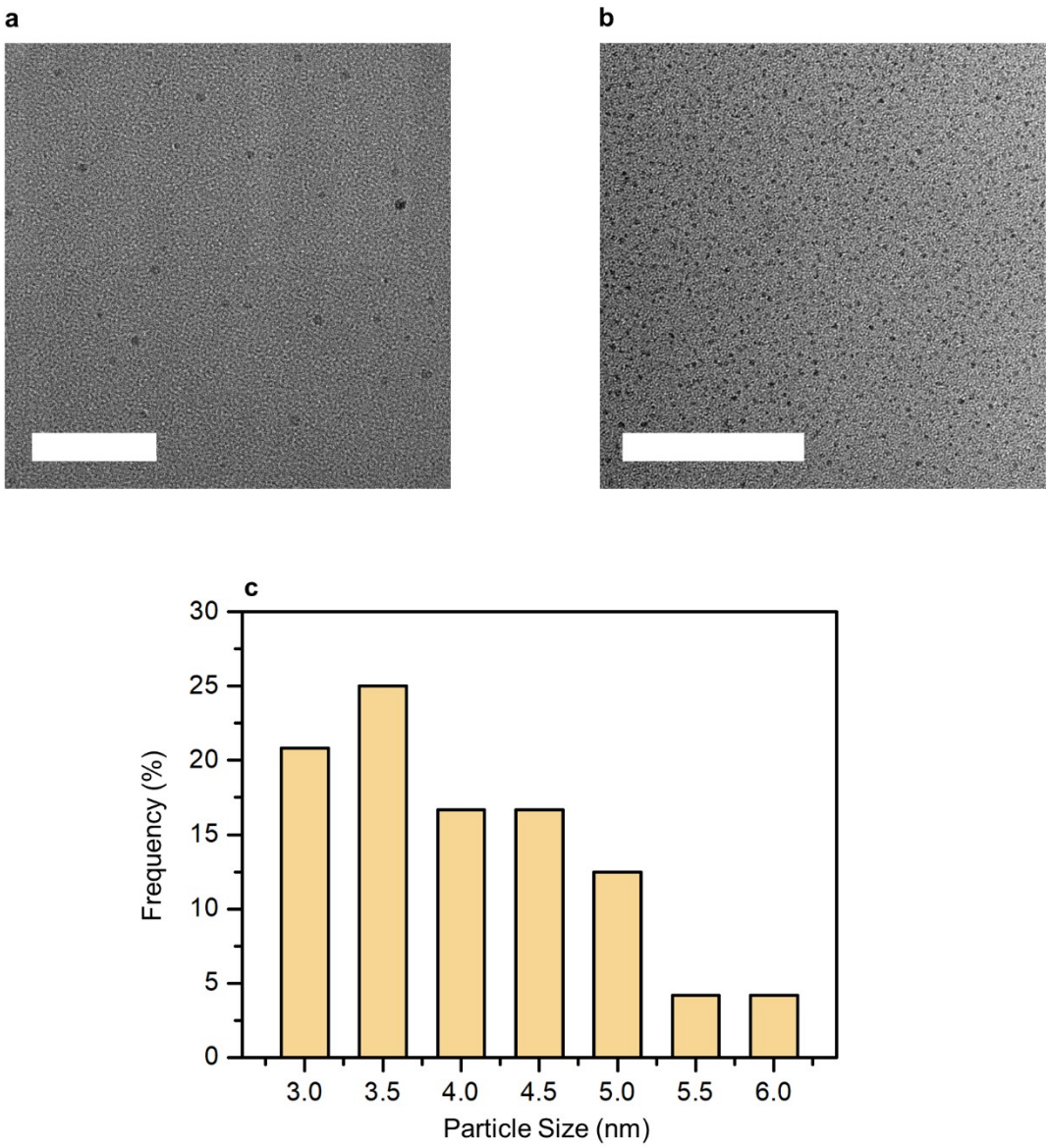

Fig. S3. TEM images of GE-CDs at different magnifications: (a) 50 and (b) 100 nm scale bars. (c) The particle size distribution of GE-CDs.

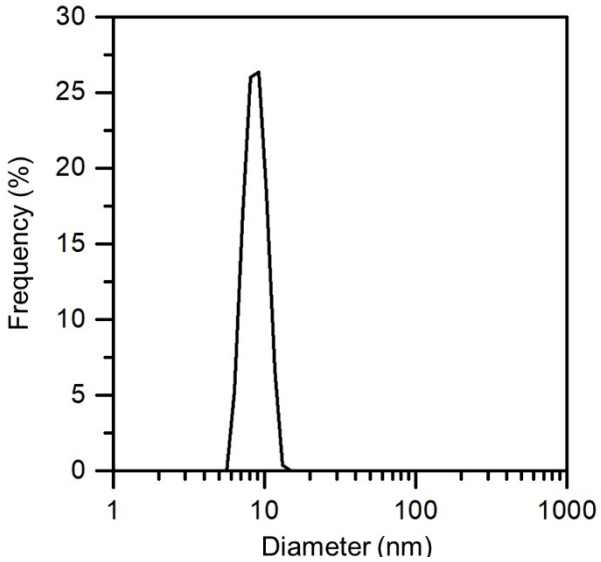

Fig. S4. DLS size distribution curve of GE-CDs.

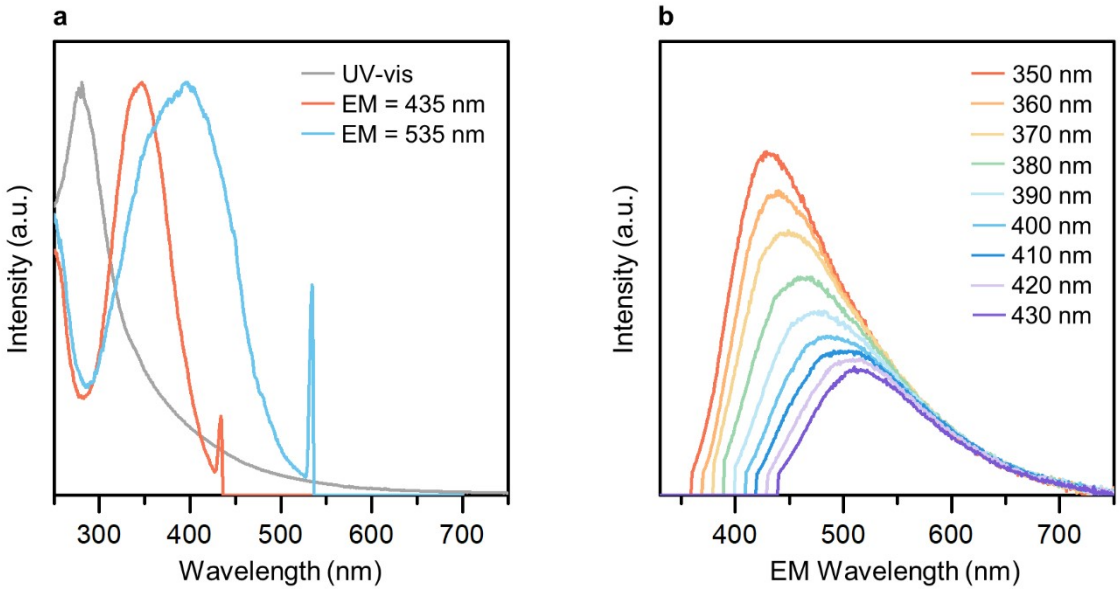

Fig. S5. (a) Normalized UV-vis absorption and PLE spectra of G-CDs. (b) PL emission spectra of G-CDs under different excitation wavelengths.

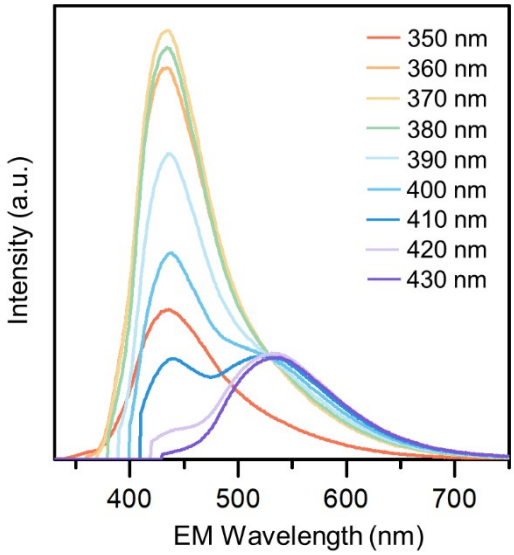

Fig. S6. PL emission spectra of GE-CDs under different excitation wavelengths.

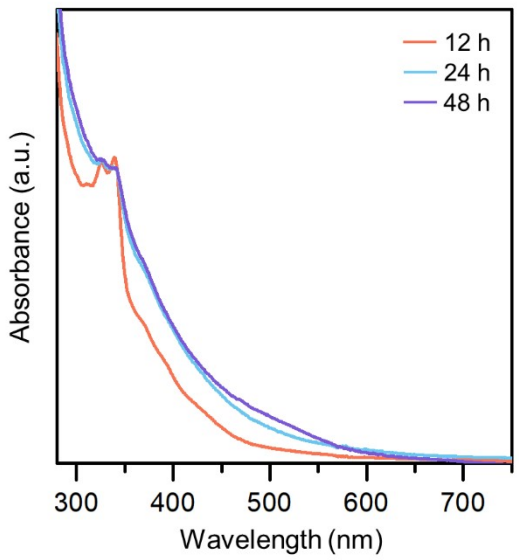

Fig. S7. UV-vis spectra of GE-CDs at different reaction times.

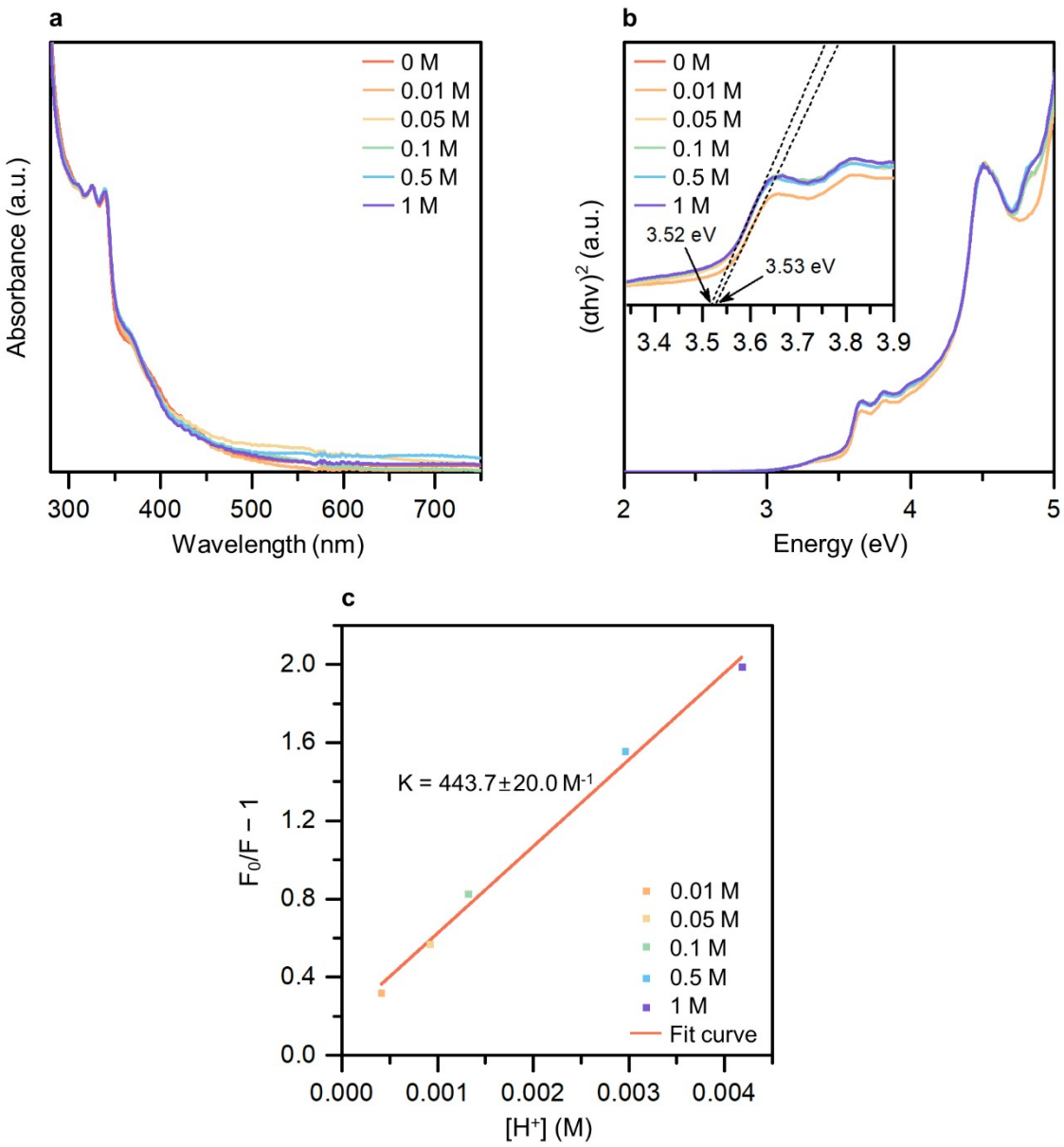

Fig. S8. (a) UV-vis spectra and (b) Tauc plots of GE-CDs in the presence of acetic acid at different concentrations. The inset shows magnified spectra of the 3.35–3.9 eV range. (c) Relative PL intensity of GE-CDs as a function of proton concentration in the presence of acetic acid.

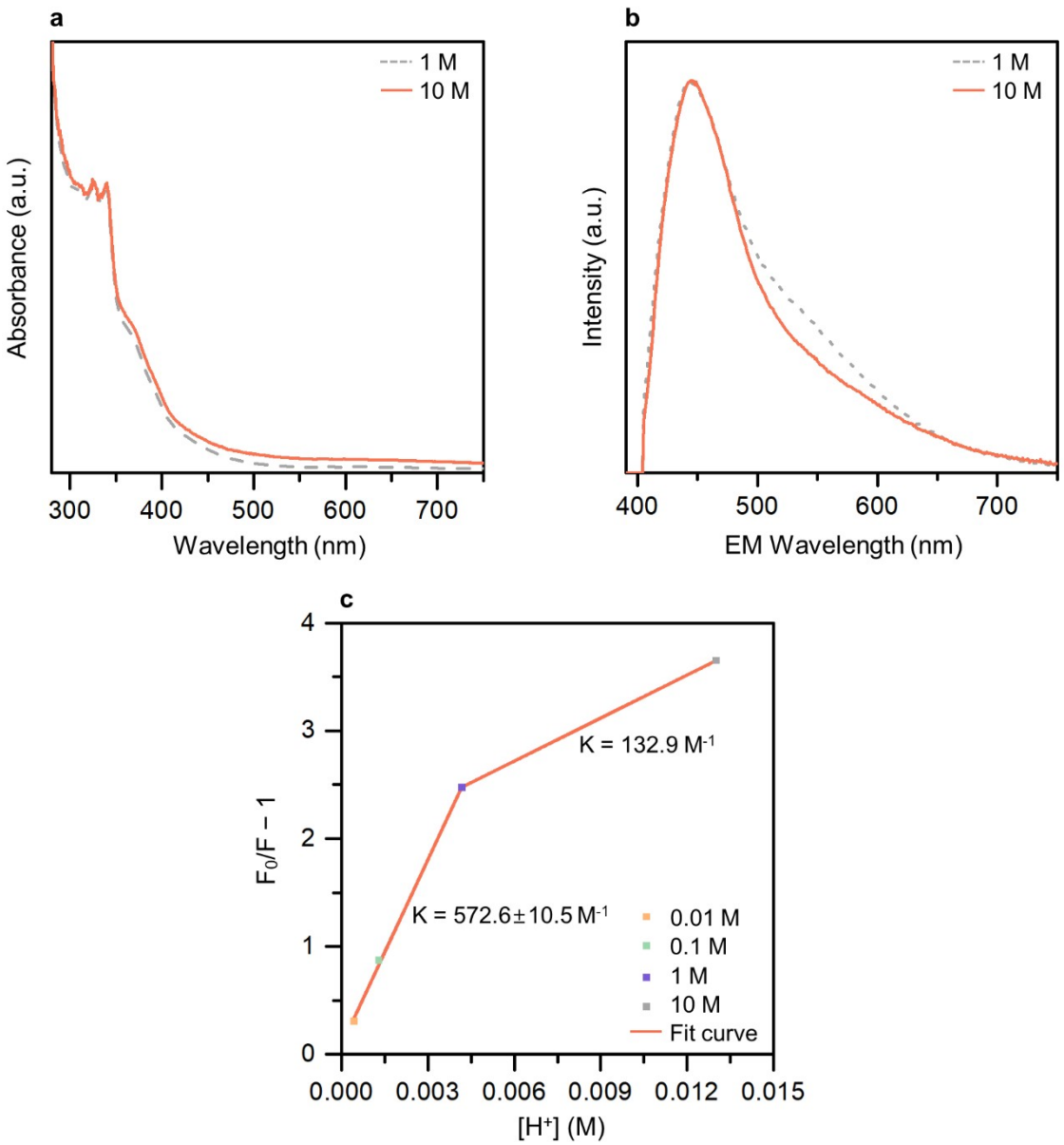

Fig. S9. (a) UV-vis spectra and (b) PL emission spectra of GE-CDs at excitation wavelength of 390 nm in the presence of acetic acid with concentrations of 1M and 10M. (c) Relative PL intensity of GE-CDs as a function of proton concentration in the presence of acetic acid.

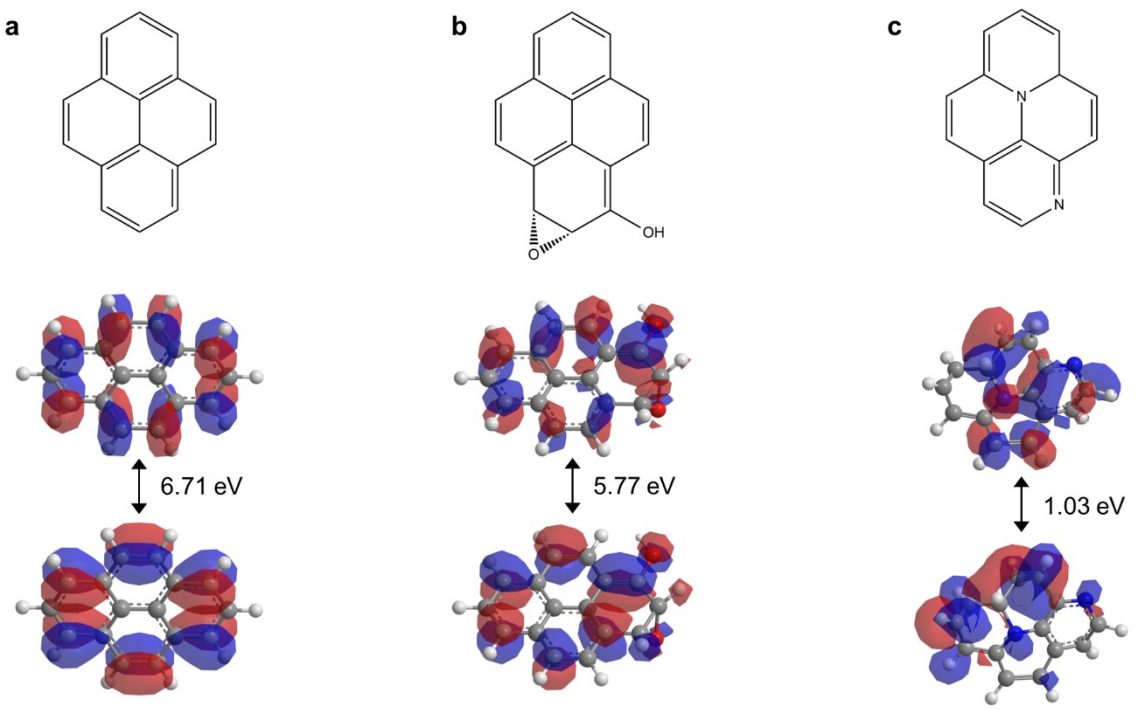

Fig. S10. Molecular orbital energy levels and band structures of (a) pyrene, (b) oxygenic pyrene, and (c) pyrene with graphitic nitrogen (grey: carbon, blue: nitrogen, red: oxygen, white: hydrogen).

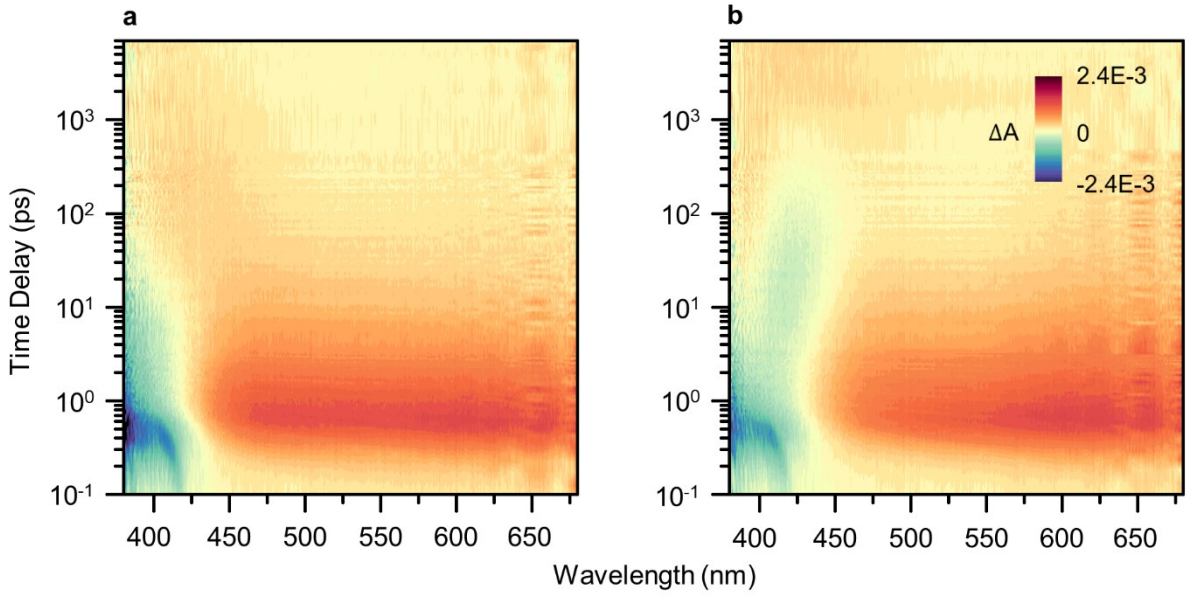

Fig. S11. TA contour maps of (a) G-CDs and (b) GE-CDs excited by a 360 nm pump wavelength.

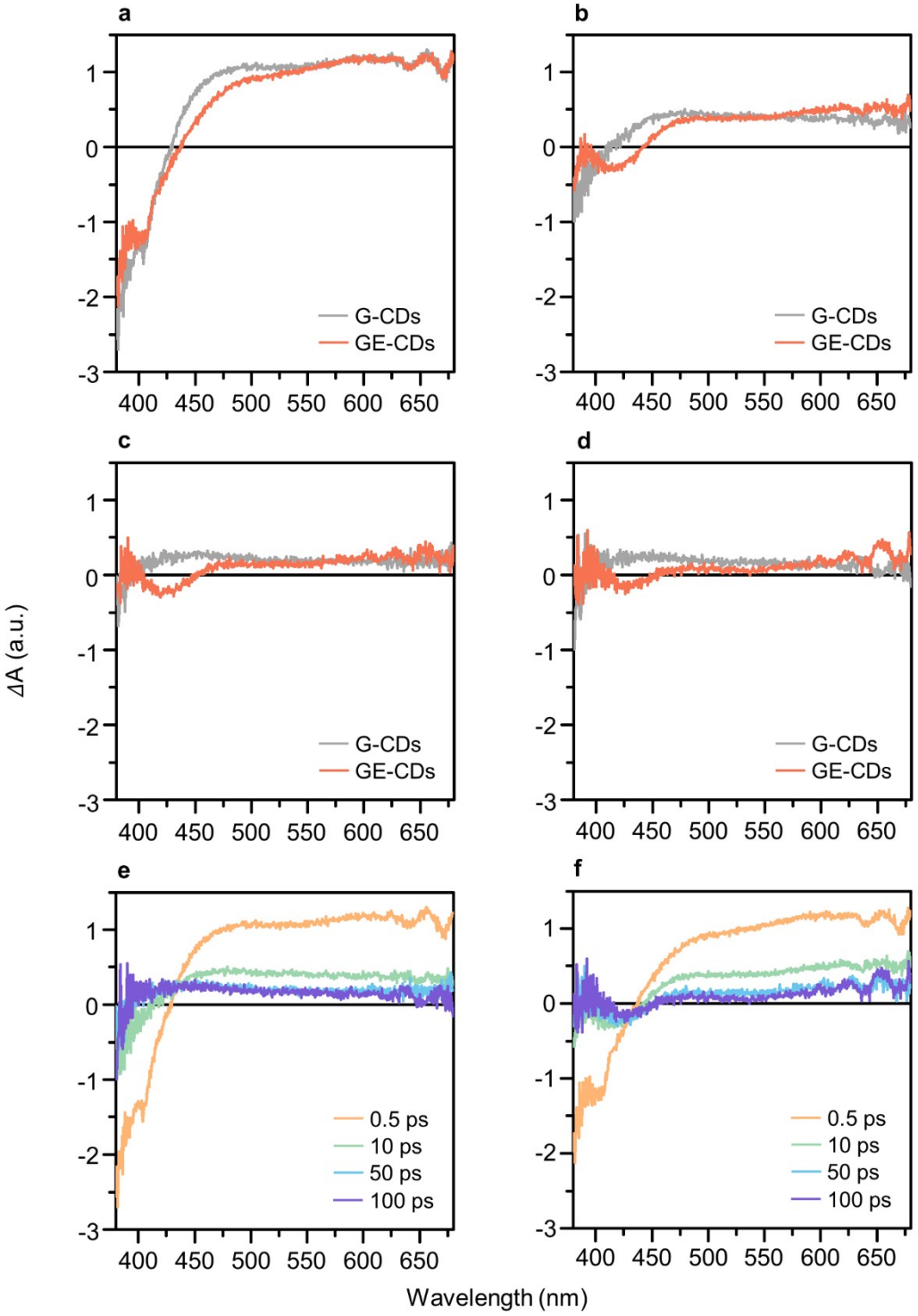

Fig. S12. Comparison in the TA spectra of G-CDs and GE-CDs at time delays of (a) 0.5 ps, (b) 10 ps, (c) 50 ps, and (d) 100 ps. TA spectra of (e) G-CDs and (f) GE-CDs at different delay times and excitation wavelength of 360 nm.

Table S1. TA fitting parameters of the G-CDs and GE-CDs under different excitation wavelengths at (a) 435 nm and (b) 535 nm probe wavelength.

(a)

Sample	Excitation (nm)	τ (ps)
G-CDs	360	2.31
GE-CDs	360	5.20

(b)

Sample	Excitation (nm)	τ_1 (ps)	τ_2 (ps)
G-CDs	360	1.73	-
	440	5.03	-
GE-CDs	360	1.6	16.1
	440	20.0	-

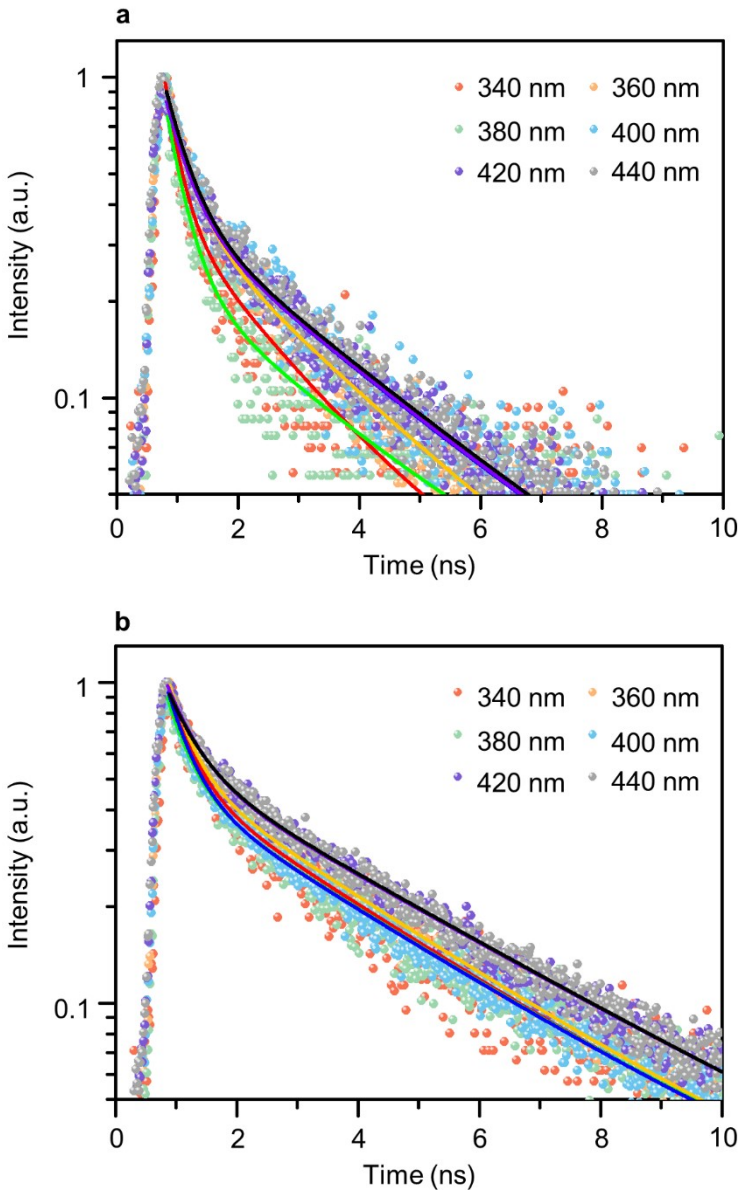

Fig. S13. Normalized PL intensities of (a) G-CDs and (b) GE-CDs at 535 nm emission as a function of pump exposure time under excitation at 340, 360, 380, 400, 420, and 440 nm. The solid lines in deep colors indicate exponential decay fits.

Table S2. TRPL fitting parameters for G-CDs and GE-CDs under different excitation wavelengths at 535 nm emission wavelength.

Sample	Excitation (nm)	τ_N (ns)	τ_R (ns)
G-CDs	340	0.24	1.80
	360	0.37	2.38
	380	0.31	2.55
	400	0.37	2.72
	420	0.38	2.75
	440	0.38	2.77
GE-CDs	340	0.38	3.44
	360	0.38	3.43
	380	0.38	3.52
	400	0.38	3.54
	420	0.47	3.96
	440	0.49	3.97

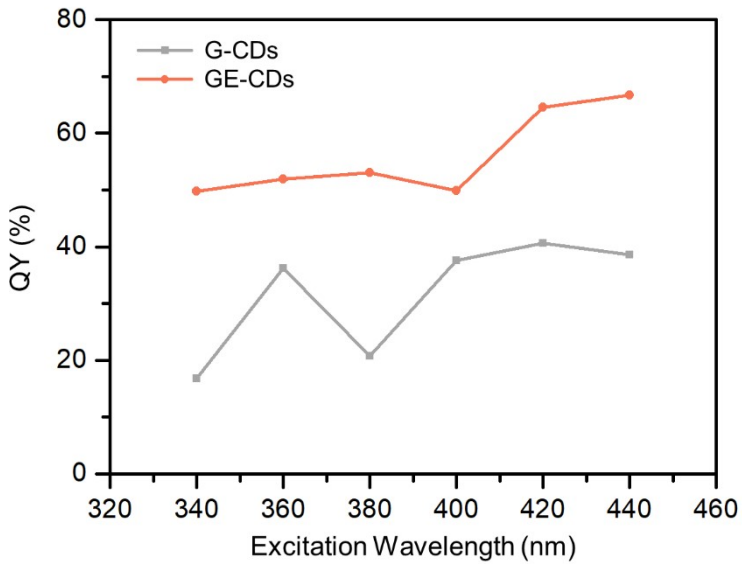

Fig. S14. Theoretical calculations of PL QYs for G-CDs and GE-CDs at various excitation wavelengths.

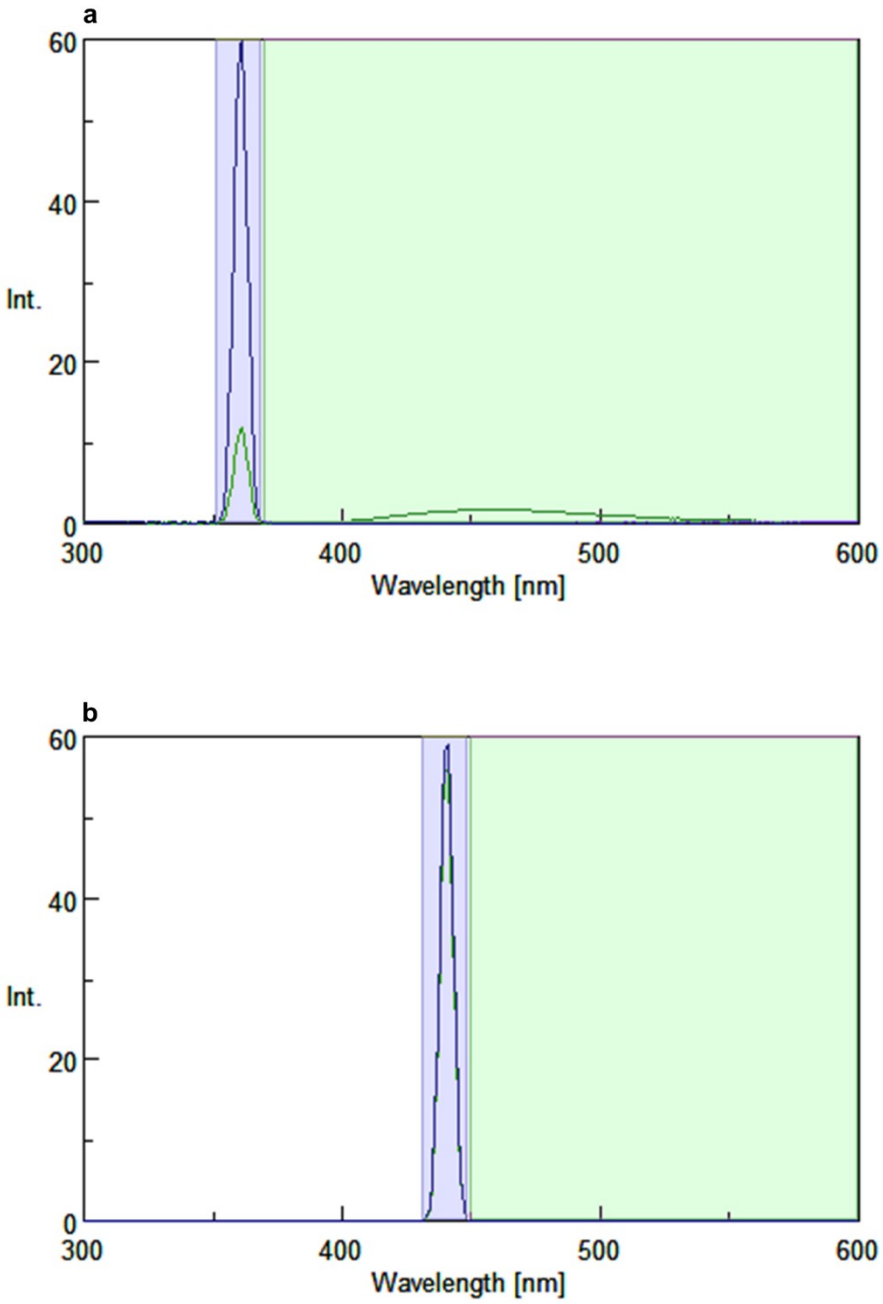

Excitation Wavelength (nm)	Absorptance (%)	Ext. Quantum Efficiency (%)	Int. Quantum Efficiency (%)	Incident Light	Fluorescence	Scattering
360	79.7	46.377	58.189	398.39	184.76	80.87
440	5.931	3.105	52.354	385.72	11.98	362.85

Fig. S15. Absolute QY measurements of GE-CDs at excitation wavelengths of (a) 360 and (b) 440 nm utilizing the Jasco Spectra Manager II software.

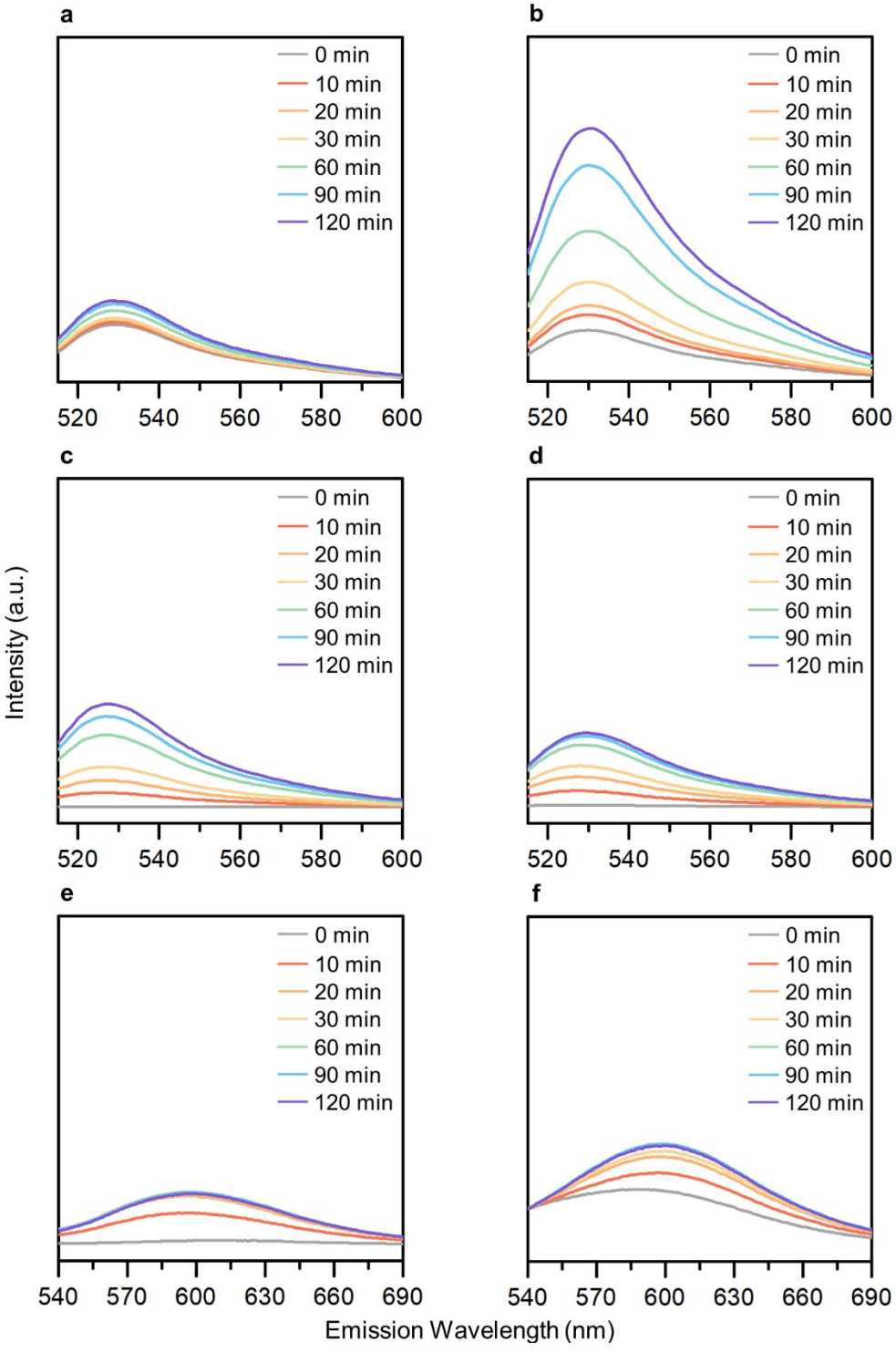

Fig. S16. The PL spectra of (a, c, e) pure water and (b, d, f) GE-CDs (0.5 mg/mL) under UV radiation (254 nm) with (a, b) SOSG, (c, d) DHR 123, and (e, f) Red Fluorometric ROS Kit for a duration of 0–120 min.

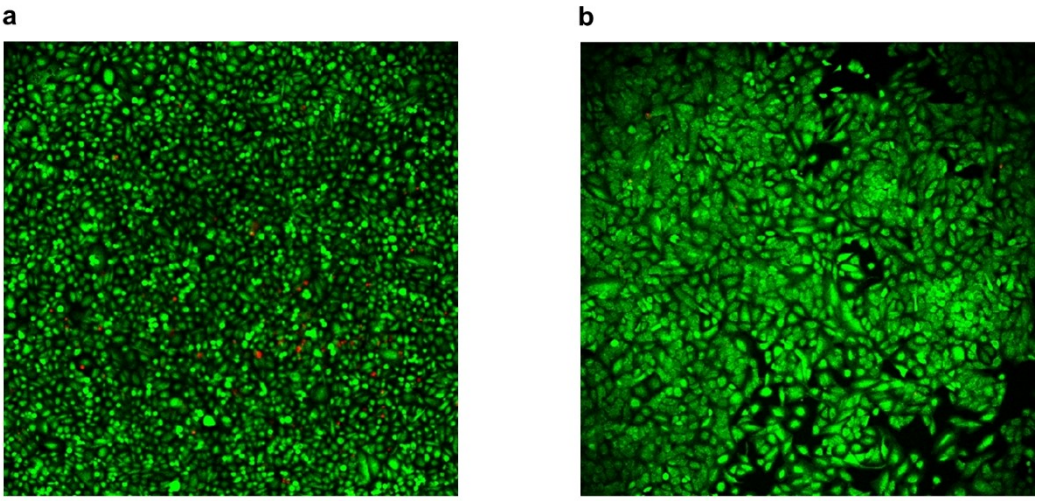

Fig. S17. Fluorescence images of calcein AM- and PI-co-stained control groups of (a) PC3 and (b) A549 cells irradiated only with the laser.